Rev.Adv.Mater.Sci. 25 (2010) 209-218

THE ANALYSIS OF THE EFFECT OF MICROSTRUCTURE PARAMETERS ON THE ABILITY TO DEVELOP HIGH-STRENGTH STATES AND PECULIARITIES OF DEFORMATION BEHAVIOR OF Al 1570 ALLOY

I. V. Alexandrov and R. G. Chembarisova

Department of Physics, Ufa State Aviation Technical University, 12 K. Marx St., Ufa, 450000, Russia

Received: December 15, 2009

Abstract. The role of various microstructure parameters in developing the experimentally ultra-high strength of nanostructured aluminum-magnesium Al 1570 (Al-5.7Mg-0.32Sc-0.4Mn wt.%) alloy has been analyzed here. It was demonstrated that the main factors, which determined the alloy strength, are the grain size, the dislocation density and the segregation of magnesium atoms from the solid solution of the alloy into the grain boundary area. We have also received the cardinal values of the dislocation pinning stress by the magnesium atoms, as well as the stress conditioned by the material hardening as the result of dislocation interaction. The analysis of the deformation mechanisms has been resulted here too.

1. INTRODUCTION

It's a common knowledge that microstructure change by applying various techniques of thermomechanical treatment allows managing the structural strength of the metallic materials [1-3]. In connection with this, the material hardening takes place due to the microstructure refinement, increase of the defect level in the crystalline structure and the impurity influence.

The strength improvement of the polycrystalline materials with the reduction of the grain size follows the empirical Hall-Petch (HP) law, binding the yield limit with an average grain size in polycrystalline materials [4,5] with the help of the following equation

$$\sigma = \sigma_0 + Kd^{-1/2}, \quad (1)$$

where σ_0 - is the friction stress, experienced by the edge dislocations during their slip in the crystal lattice inside the grains (the yield limit of a single crystal), K – is the HP coefficient, d – is the grain size. The HP relation is carried out in a wide range of the grain sizes from 10÷15 nm to 100 μm [5,6].

However, if the grain size is reducing less than 10÷15 nm, the deviations from the HP law start to occur here. Therefore, the yield limit at the temperatures (0.2÷0.3) T_m appears to be lower than the one, which has been predicted with the help of this law [7]. The deviations from the HP law occurred both in micro-crystalline metallic [8] and in ceramic [9] materials at temperatures (0.4÷0.5) T_m with the grain

Corresponding author: I. V. Alexandrov, e-mail: iva@mail.rb.ru

size less than a certain critical value 1÷10 μm. Simultaneously the peculiarities of the microstructure and the deformation mechanisms, which are characteristic of the materials with the small grain size developing the deviations from the HP law, have not been studied well yet.

The problem gets more complicated when we are concerned with the bulk nanostructured (NS) materials, obtained by the severe plastic deformation (SPD) methods [10]. As is well-known, these methods lead to the formation of highly non-equilibrium NS states. The management by the level of microstructure non-equilibrium provides quite different strength with the same grain size and the ability to develop the different levels strength properties of the bulk NS materials, obtained by the SPD methods.

Among the bulk metallic NS materials, received by the SPD methods, the aluminum-magnesium alloys take a special place. In the common case the interest to these alloys is raised by their high corrosion resistance and good weldability. In connection with this they are used to produce the express vessels, for instance. At the same time, the improvement of the strength properties and investigating their dependency from the grain size and other microstructure parameters are undoubtedly of great importance.

Let us mention the fact, that the strength properties of these alloys, apart from the reasons mentioned above (the grain size, the non-equilibrium of the microstructure) might influence the solid solution hardening, disperse particles, Mg atom segregations [1-3,11-14].

According to the recently obtained experimental findings [2,3], the Al-Mg alloys in submicrocrystalline (SMC) state show higher strength in comparison with its coarse-grained (CG) analogue.

So, in paper [2] the Al 1570 (Al-5.7Mg-0.32Sc-0.4Mn wt.%) alloy, taken in CG state, annealed at 380 °C, was subjected to high pressure torsion (HPT) at room temperature (RT), and at 100 °C and 200 °C. As a result, the states were formed with the grain sizes 130 ±10 nm, and 210±7 nm with mainly high-angle grain boundaries (GBs). Moreover, the disperse particles with size less than 10 nm have been found in the microstructure of an alloy, given both in an initial state and after HPT at the indicated temperatures. The phase analysis has pointed out the belonging of these disperse particles to Al_3Sc-phase, segregated during annealing of an ingot in an initial state.

Sc is a very efficient microstructure modifier, developing small coherent particles in an Al matrix [1]. The particles of the Al_3Sc-phase considerably preserve the grain size from the growth and increase the alloy strength. The structure thermostability increases too. The latest one stays fine-grained during annealing up to 500 °C [1].

In paper [1] it is demonstrated that the change of the Mg content in the Al-Mg alloys and their SPD conditions by the equal-channel angular pressing (ECAP) influences greatly the developing microstructures and the obtained strength properties. The yield limit is increasing as well as the Mg concentration (while the Sc concentration stays constant) in the samples with SMC structure.

In spite of the fact that the grain sizes are approximately equal (340 and 330 nm correspondingly) in the samples with the Mg concentration 4.5% and 1.5%, the yield limits are 370 and 280 MPa correspondingly. The yield limit has fallen down to 230 MPa in the microcrystalline alloy with the grain size approximately equal to 12 μm and the concentration of Mg equal to 6%, while the ductility of the sample has increased considerably.

One can suggest that the yield limit has increased on account of the Mg segregation at the GBs in a SMC alloy at the processing temperatures equal to 140 °C and 160 °C correspondingly. The yield limit of the samples is determined not only by the grain size, but also depends on the microstructure peculiarities, developed in the process of thermomechanical treatment. One can also suggest that the yield limit increase in the investigated alloys is conditioned by the presence of the Al_3Sc-phase particles. This phase can pin the dislocations efficiently, therefore, it can contribute to the material hardening.

The coherent fine Al_3Sc particles are hard to deform by cold working because of the high yield limit and relatively low ductility. The grain-matrix is ductile, whereas the inclusions are rigid and strong [13].

The high values of the yield limit have been observed in the nanostructured Al-7.5%Mg alloy [3]. The alloy has been obtained the following way. Spray atomized alloy powders were cryomilled. The cryomilled powders were consolidated and extruded for tensile testing and microstructural analysis. As a result the samples with the grain size 100÷300 nm and the yield limit equal to 641 MPa have been obtained. High strength in this case has been achieved due to the small grain sizes. At the same time, developing the bimodal structures is the re-

sult of the mixing of the refined powder with 15% and 30% unmilled powder, which allowed getting the samples with the improved ductility and quite a high yield limit (630 MPa and 554 MPa respectively).

In paper [2] the non-monotonic character of the dependency $\sigma_y = f(d^{-1/2})$ in the area of micron and submicron grain sizes in the Al 1570 alloy has been deduced experimentally. In this case, the possibility to obtain the ultrahigh-strength state with the yield limit higher than the one, which was predicted with the help of the HP law, has been demonstrated here. It has been suggested that reasons for developing the ultrahigh-strength SMC state are the peculiarities of the solid solution dissociation, followed by the dynamic ageing in the process of HPT, β-phase development and segregation of the Mg atoms out of the crystalline lattice into the GB area.

The aims of this paper are obtaining the model dependencies $\sigma = f(d^{-1/2})$, their correlation with the analogous experimental dependency and interpretation of the mechanisms, developing the ultrahigh-strength states in NS Al-Mg alloys on the example of the Al 1570 alloy.

2. THE BASIC PROVISIONS OF THE MODEL

The dislocation-based approach has been applied to get the model dependencies $\sigma = f(d^{-1/2})$. The model has been based on the concepts about dislocation hardening on account of dislocation interaction with one another and with the GBs, solid-solution hardening, hardening connected with the second phase particles (Al_3Sc-phase, possibly coherent β'-phase and non-coherent β-phase), hardening on account of impurity atmospheres development on the dislocations, as well as the experimental curves $\sigma = f(d^{-1/2})$ [4,12,15].

The yield stress in the model is determined according to the well-known Taylor relationship [16] to strengthen the crystalline material as the result of dislocation interaction with each other and the other obstacles:

$$\sigma = \sigma_0 + M\alpha Gb\sqrt{\rho}, \tag{2}$$

where σ_0 – the friction stress, experienced by the dislocations during their interaction with the lattice defects and various obstacles of non-deformation origin (which is necessary for the dislocation motion with the absence of other dislocations), M – the Taylor factor for polycrystals under the conditions of uniaxial deformation by extension ($M = 3.05$), α – the coefficient of dislocation interaction, G – the shear modulus ($G = 27$ GPa), b – the Burgers vector value ($b = 0.286 \times 10^{-9}$ m), ρ – the average dislocation density in the sample.

Value σ_0 has been determined by the extrapolation of the certain experimental dependency $\sigma_y = f(d^{-1/2})$ toward the value $d^{-1/2} = 0$.

Considering the hardening on account of developing the impurity atmospheres on the dislocations we finally get

$$\sigma = \sigma_0 + M\alpha Gb\sqrt{\rho} + \tau_s M = \sigma_0 + \sigma_\rho + \sigma_s, \tag{3}$$

τ_s – the pinning stress (the resolved shear stress of the dislocation slip).

In paper [17] they have got the time law of the extra-strength change, related to the impurity accumulation depending on the time in the neighborhood of the edge dislocation in Al-Mg alloys. The pinning stress τ_s is determined in the following way:

$$\begin{aligned}
&\tau_s = \Delta\tau_0(1 - e^{-t/t_s}),\\
&t_s = (6\cosh(\Delta\bar{W}/2kT)\Gamma_c)^{-1},\\
&\Gamma_c = \nu_0 e^{-\Delta H_c/kT},\\
&\Delta\tau_0 = 2\alpha' c_0 \Delta\bar{W}\tanh(\Delta\bar{W}/2kT)/\sqrt{3}b^3,
\end{aligned} \tag{4}$$

where $\Delta\tau_0$ - the strength prefactor, $\Delta\bar{W} \approx 0.13$ eV - the average pinning energy difference between the core tension and compression planes, $\nu_0 \approx 10^{13}\ s^{-1}$ - the Debye frequency, $\Delta H_c \approx 0.97$ eV – the average activation enthalpy for transitions from tension to compression, $\alpha' \approx 0.56$ – the parameter, depending on the thermodynamic driving force $\Delta W \sim 0.13 \pm 0.02$ and value $\Delta\bar{W}$, c_0 – the bulk solute concentration, k – the Boltzmann constant, T – the temperature.

The dislocation density change in the fine-grained materials in the process of deformation can be described by the equation [18,19]:

$$\frac{d\rho}{dt} = \frac{\beta\dot{\gamma}}{bd} - \frac{\rho}{t_a}, \tag{5}$$

where $\dot{\gamma}$ – is the deformation rate, β – is the coefficient, which value is equal ≈1 in case of the action of mechanism limiting the free dislocation run [4], t_a – is the characteristic time of dislocation annihilation in the grain boundaries [19-23], which value is calculated according to the formula:

$$t_a = \frac{d^2 kT}{4D_{gb}Gb^3} = \frac{d^2}{8B'} \tag{6}$$

where,

$$B' = \frac{D_{gb} b^3 G}{2kT},$$

D_{gb} – the coefficient of grain-boundary diffusion.

As it is shown in paper [19], the flow stress in the fine-grained structures can be determined only by the grain sizes and by the properties of their boundaries as the sources and sinks for dislocations. Besides, the efficiency of the dislocation sources and sinks at low temperatures becomes lower too [24,25], but it can increase along with the temperature raise under the condition that annihilation of dislocations with the help of the grain-boundary diffusion takes place in the GBs. Thereafter, the first term in the right part of the expression (5) features the dislocation accumulation in consequence of the GB presence, the second one – the dislocation annihilation in the GBs, due to the increase of the volume fraction of the GBs and diffusive processes intensification in them as the result of the decrease of diffusive distances [23].

The annihilation of the edge dislocations in the GBs is determined by the time of their solution in the boundary, leaving into the triple junction $t_{a1}=l^3/\eta_1 b D_{gb}$ [17,19] and the time of the paired annihilation of dislocations of the opposite sign in them $t_{a2}=l^2/4\eta_2 D_{gb}$ [19-23], $\eta_1 \approx \eta_2 \approx Gb^3/kT$.

Assuming the fact that the pointed out processes are taking place independently of one another, and their specific times depend on the maximum distance in the boundary $l=d$, Eq. (5), describing the change of an average dislocation density depending on the slip deformation $\gamma = M\varepsilon$, has been put down as [19]:

$$\frac{d\rho}{d\gamma} = \frac{\beta}{bd} - \frac{\rho}{t_a \dot{\gamma}} = \frac{\beta}{bd} - (k_{a1} + k_{a2})\rho, \qquad (7)$$

where

$$k_{a1} = \frac{1}{t_{a1}\dot{\gamma}}, \quad k_{a2} = \frac{1}{t_{a2}\dot{\gamma}}.$$

Eq. (6) in case of the activity of the paired annihilation transfers into the expression, coinciding with t_{a2} [23]:

$$t_a = t_{a2} = \frac{kTd^2}{4D_{gb}Gb^3}. \qquad (8)$$

The estimates of the annihilation coefficient k_{a2} with the values t_{a2}, determined at d = 130 nm and d = 210 nm, yield the values 1.7 and 0.65 respectively. In the first case the annihilation time is equal to ≈ 1939 s, in the second one - 5060 s.

At the deformation rate $\dot{\varepsilon} = 10^{-4}$ s^{-1} the annihilation takes place at the deformations ≈ 0.2 and ≈ 0.5 respectively. It has been assumed, that the activation energy of the GB diffusion is $E_{gb} \approx 0.5E_b$ [14], the activation energy of the bulk diffusion is $E_b \approx 16\,kT_m$ [26]. The coefficient of the GB diffusion is $D_{gb}=D_0\exp(-E_{gb}/kT)$, $D_0 = b^2\nu_v$. Besides the frequency of the vacancy jumps is 2x10^{-3} times more than the one for interstitial atoms: $\nu_u \approx 2\text{x}10^{-3}\nu_0$. At T = 293K, T_m = 930K, $D_{gb} \approx 1.39\times10^{-20}$ m^{2}s^{-1}.

If the annihilation of edge dislocations in GBs is determined by the time of their solution in the boundary, the annihilation time in Eq. (6) coincides with t_{a1} [23]:

$$t_a = t_{a1} = \frac{kTd^3}{D_{gb}Gb^4}. \qquad (9)$$

The comparison of expressions (9) and (8) shows that the time of the paired annihilation (8) is $4d/b$ times less than the time of the dislocation solution in the boundary. The coefficient of the paired annihilation of dislocations is 1818 and 2937 as much as the coefficient of the isolated dislocations annihilation in the boundary with the grain size 130 nm and 210 nm correspondingly. That is why the characteristic annihilation time makes sense of the annihilation time of the paired dislocations with the opposite signs in GBs in Eqs. (5) and (7). The annihilation coefficient of the single dislocations in the boundary can then be ignored.

Integrating Eq. (5), the evolution of the dislocation density can be expressed analytically in the form of the dependency

$$\rho = \rho^*\left(1 - \left(1 - \frac{\rho_0}{\rho^*}\right)e^{-\gamma/\gamma^*}\right), \qquad (10)$$

where

$\rho^* = \frac{t_{a2}\dot{\gamma}}{bd}$, $\gamma^* = t_{a2}\dot{\gamma}$, ρ_0 - is the initial dislocation density. So, the crystalline material hardening will follow the law

$$\sigma = \sigma_0 + M\alpha Gb(\rho^*)^{1/2}\left(1 - \left(1 - \frac{\rho_0}{\rho^*}\right)e^{-\gamma/\gamma^*}\right) + \tau_s M. \qquad (11)$$

In other words, the non-monotonous dependency of the flow stress from the grain size can be observed here.

In case of CG polycrystalline materials the change of the dislocation density depending on the shear deformation can be described with the help of the equation [19,22]

$$\frac{d\rho}{d\gamma} = \frac{\beta}{bd} + \frac{1}{b\lambda_m} + k_f\rho^{1/2} - k_{cs}\rho - \frac{\rho}{\dot{\gamma}t_a}. \qquad (12)$$

The second term in Eq. (12) features the dislocation accumulation at obstacles during the double cross slip (DCS) of the screw dislocations, the third term – on the forest dislocations, which present obstacles of deformation origin. λ_m describes the length of free dislocation run between the two events of DCS. k_f is the coefficient of dislocation multiplication on the forest dislocations.

According to the experimental data b/λ_m can take values from $b/\lambda_m = 1\text{x}10^{-2}(\sigma_0/M)/G$ to $b/\lambda_m = 2\text{x}10^{-2}(\sigma_0/M)/G$, $bk_f = \delta_f \approx 10^{-2}$ [27,28]. It is suggested that a reduction of the dislocation density takes place in addition to the screw dislocation annihilation during the DCS, featured by the annihilation coefficient k_{cs}, which value is in the interval between 2 and 10, according to the experimental data [28,29] in case of FCC – metals in the temperature range of $(0.1\div0.3)\,T_m$ and depending on the energy of the stacking fault. However, in case of the initial annealed state, the paired dislocation annihilation can be ignored. Then the annihilation of the single dislocations in the GBs can be ignored too. In fact, at $d \approx 500$ μm $k_{a2} \approx 1.1\times10^{-7}$, $k_{a1} \approx 1.6\times10^{-14}$. During the calculations it was assumed that $k_{cs} \approx 2.1$ [19], $1/b\lambda_m \approx 59.4\times10^{13}$ m^{-2}, $\sigma_0 \approx 200$ MPa. The flow stress has been calculated according to Eq. (3).

3. THE RESULTS OF SIMULATION AND THEIR DISCUSSION

The experimental data concerning hot-pressed Al 1570 alloy, annealed at 380 °C during 2 hours CG state, as well as NS states of this alloy, obtained by the following HPT at RT (NS 1 state), at 100 °C (NS 2 state) and 200 °C (NS 3 state) have been used for numerical modeling observed on the experiment of the plastic deformation regularities of the Al-Mg alloys [2]. The above mentioned NS states differed by the grain size, the density of the crystal lattice defects, the crystal lattice parameter and the strength properties (Table 1). The mechanical tensile tests were carried out at RT at the strain rate 10^{-4} s^{-1} [2].

The authors [2] have used annealing of the alloy in an initial state to provide the utmost Mg solution in the matrix, the maximum solid solution hardening for analysis of the influence of the dimensional effect only on the strength properties of the alloy.

In the process of solid solution development the crystal lattice of Al strains as a result of the various size of the matrix atoms and the impurity atoms. In the process of plastic deformation the dislocations overcome the resistance of the crystal lattice during their movement. Therefore, this factor contributes to the deformation resistance. That is why the solid solution hardening should also be considered as an important factor, providing the strength of the alloy under study.

In paper [2] the segregation of the particles of Al_3Sc-phase in the process of homogenizing annealing of the initial sample has been revealed here. Similar segregations were observed after HPT treatment as well [2]. Besides, the probability of the disperse particle segregation of β- phase (Al_3Mg_2) (the coherent ones, or with the disrupted coherence) and their contribution into the strain hardening cannot be excluded here, as the HPT was realized at elevated temperatures. The segregation of the Mg atoms out of the solid solution into the GBs area took place in the HPT process [2]. The segregations of atoms can lead to a strengthening effect, which must be considered while modeling.

In the SPD process the structure with the high dislocation density has been developed. The introduction of a great number of dislocations into the crystal lattice also leads to strain hardening. So, in

Table 1. The experimentally obtained parameter values.

States	*d*, nm	ρ, m^{-2}	*a*, Å	σ_y, MPa	σ_u, MPa	δ, %
CG	-	-	4.0765±0.0001	231±9	376±10	17±1
NS 1	130±10	$5.1\cdot10^{14}$	4.0692±0.0003	905±31	950±35	4.7±0,3
NS 2	130±10	$3.4\cdot10^{14}$	4.0682±0.0002	865±25	890±18	4.0±0,4
NS 3	210±7	$5.6\cdot10^{12}$	4.0685±0.0001	845±33	845±33	0

the process of modeling it is necessary to take into consideration the possible contribution of the all the above mentioned factors into the strain hardening of the alloy.

The authors of paper [2] considered that, in case if the annealing of the alloy samples provides the utmost Mg solution in the crystal lattice, the hardening of the alloy in the result of HPT should be provided only on the account of the microstructure refinement. However, the experimental dependency $\sigma = f(d^{-1/2})$ has revealed deviations from the HP law. The alloy subjected to HPT has appeared to be in an ultrahard state. To reveal the factors determining the strength and the ductility of the alloy samples, subjected to HPT, the analysis on the basis of the model described in part 2 has been carried out in the present paper.

Eqs. (10) and (12) allowed analyzing the character of the dependency of the yield stress (3) at the strain rate 0.2% from the grain size. The contribution of the different factors considered in Eq. (3) into the total yield stress of the alloy in various structure states has been studied here. Let us start our consideration with the contribution of a defect microstructure.

In case of a CG state of an alloy the dislocation density, as follows from Eq. (12), depends on the grain size according to the law $\rho \sim 1/d$. Therefore,

$$\sigma_\rho \sim d^{-1/2}. \tag{13}$$

Eq. (10) describing the dislocation density evolution in NS states can be demonstrated in the following form

$$\rho = \rho_0^* d\left(1 - \left(1 - \frac{\rho_0}{\rho_0^* d}\right) e^{-(d_v/d)^2}\right), \tag{14}$$

where

$$\rho_0^* = \frac{kT\dot{\gamma}}{4D_{gb}Gb^4},$$

$$\gamma_0^* = \frac{kT\dot{\gamma}}{4D_{gb}Gb^3},$$

$$d_v = \left(\frac{\gamma}{\gamma_0^*}\right)^{1/2}.$$

Then the contribution to the total stress, according to Eq. (3), will depend on the grain size, in respect with the law

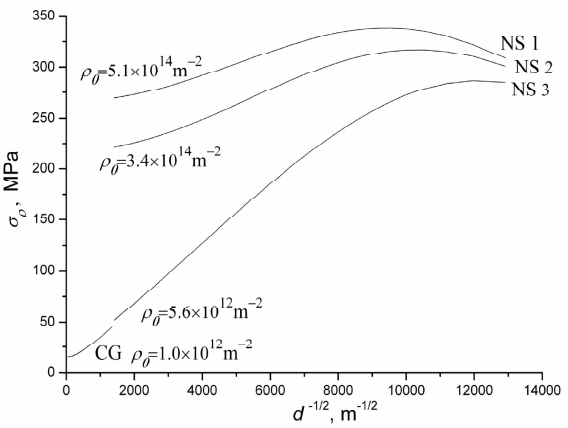

Fig. 1. The contribution into the flow limit of the dislocation hardening alloy σ_c (at the strain degree ε=0.002) depending from $d^{-1/2}$ at different values of the initial dislocation density.

$$\sigma_\rho = M\alpha Gb(\rho_0^*)^{1/2} d^{1/2} \times \left(1 - \left(1 - \frac{\rho_0}{\rho_0^* d}\right) e^{-(d_v/d)^2}\right)^{1/2}. \tag{15}$$

Fig. 1 presents the dependency of the second term contribution of Eq. (3) into the yield limit from $d^{-1/2}$ in the CG state and at different values of the initial dislocation density ρ_0 in NS states.

As follows from Fig. 1, the more defects are in the microstructure, the higher is the flow limit at the assigned value of the grain sizes. While the grain size is decreasing, the yield limit increases, achieving its highest value only in the field of very small grain sizes. Thus, the less is the initial dislocation density ρ_0, the less is the average grain size at which the flow limit obtains its maximum. GBs in ultrafine grained and nanocrystalline materials perform not only the function of the limitation of the dislocation run, which brings to dislocation accumulation in the grains, but they are the dislocation sinks and sources as well. The dislocation accumulation leads to material strength, whereas the annihilation brings to its softening. That is why the maximum appearance in the dependency $\sigma_y = f(d^{-1/2})$ can be explained by annihilation process intensification in the GBs area with the help of the mechanisms of bulk or GB diffusion [19]. In fact, the values of the corresponding coefficients of the pair annihilation k_{a2} (8) and the single dislocation annihilation k_{a1} (9) with the grain size, for instance, 15 nm leads to the val-

ues k_{a2}≈127 and k_{a1}≈0.55. These values are much more than the values obtained for SMC states (k_{a2}≈1.7 at d = 130 nm and k_{a2}≈0.65 at d = 210 nm and k_{a1}≈9.4×10^{-4}, k_{a1} ≈ 2.2×10^{-4} respectively).

In case of CG and SMC states of the samples the direct HP dependency can be observed here. Herein, in case of CG state the mechanisms of dislocation multiplication on the forest dislocations and the obstacles of non-deformational origin can be realized. Therefore, the diffusion mechanisms of the dislocation annihilation can be ignored at low and moderate temperatures. The corresponding results have been presented in the form of model points in Fig. 2. It is obvious that in the CG state the influence of deformation processes on the stress dependency σ_ρ from the grain sizes looks like the common HP relationship. At the same time in case of NS states this dependency is more complicated (Eq. (15)).

To find out the influence of the segregations of the Mg atoms on the flow stress (3), the stresses of dislocation pinning by the Mg atoms in the GBs area have been calculated here.

To calculate the stress τ_s with the help of the Eq. (4) the concentrations of Mg in the GB area were previously determined for the states after HPT.

As follows from the results of the X-ray analysis [2], the decrease of the crystal lattice parameter *a* took place in the process of HPT. Therefore, the implementation of the process at 100 °C has resulted in a greater reduction of the lattice parameter than at RT. The process carried out at 200 °C has completed by the inconsiderable increase of the pointed out parameter in comparison with the HPT at 100 °C (Table 1).

It is common knowledge that segregation of 1 at.% of Mg out of solid solution results in the decrease of the *a* value to 0.0046 Å [30]. In the process of HPT at RT ≈ 1.59 at.% of Mg has segregated out of the solid solution, at 200 °C ≈ 1.74 at.% of Mg. The segregated Mg atoms flow into the GBs area, as it was proved by the experimental observations [31]. As a result, in the first case the concentration of Mg in GBs became equal to ≈ 1.8×10^{28} m^{-3} (≈23.1 at.%), in the second case it was ≈ 2.9×10^{28} m^{-3} (32.8 at.%). In connection with this, the width of the GBs area was assumed to be 3 nm [32]. At Mg concentration 23.1 at.% (21.3 wt.%) Eq. (4) predicts a strength prefactor of $\Delta\tau_0$ ≈ 121 MPa. At Mg concentration 32.8 at.% (30.5 wt.%) – $\Delta\tau_0$ ≈ 173.3 MPa.

The crystal lattice parameter after the HPT at 100 °C is reduced as well in comparison with the

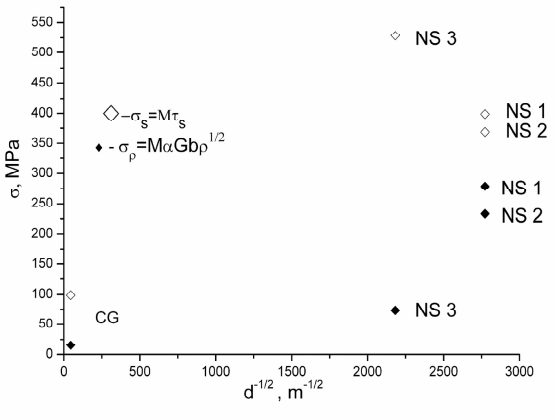

Fig. 2. Depenency of the contribution of the dislocation hardening alloy σ_p(◆) and hardening by means of dislocation interaction with the dissoluted magnesium atoms σ_s(◇) depending from $d^{-1/2}$ (at the strain degree ε=0.002).

lattice parameter in the initial state up to 0.0083 Å. So, ≈1.80 at.% of Mg has segregated out of the solid solution. The Mg concentration in GBs became equal to ≈2.0×10^{28} m^{-3} (≈24.9 at.%). The pinning stress has agreeably made - $\tau_s \approx \Delta\tau_0$ = 130.7 MPa at the Mg concentration 24.9 at.% (23 wt.%). The analysis of the model dependencies reduced at Fig. 2 shows that ultrahard states in Al alloys, obtained by the SPD method, are realized in the result of dislocation pinning by the Mg atoms, accumulated in the GBs area.

The concentration of the Mg atoms in the GBs area goes up along with the temperature increase of the processing. Therefore, the dislocation pinning stress is respectively higher. The received result is in agreement with the experimental data, according to which the atom segregations of Mg appear along the GBs in NS states [33,34].

As the number of particles of β-phase proved to be out of response limit of XRD method [2], it is possible to suggest that Mg atoms flowing into GBs stay preliminary in the solid solution, developing segregations along the GBs. This leads to the appearance of the pinning stress $\tau_s \approx \Delta\tau_0 \approx$ 32.4 MPa with the Mg concentration 5.7 wt.% in the alloy in the initial annealed state. In this state the atoms are evenly distributed inside the grains and their GBs. In the states after HPT at RT, 100 °C and 200 °C the pinning stress raises up to ≈121 MPa, ≈130.7 MPa and ≈173.3 MPa respectively on account of the increase of atom concentration in the GBs.

The grain size after HPT at RT and 100 °C is equal to 130 nm. But the pinning stress by the Mg atoms in the GBs area in the second case turned out to be higher than in the first one (Fig. 2). The rise of the pinning in the second case can be explained by enforcement of the diffusion processes together with the temperature increase, leading to the increase of the number of atoms, flowing into GBs. An inconsiderable crystal lattice parameter *a* increase after HPT at 200 °C in comparison with the state after HPT at 100 °C can be explained by the decrease of the Mg atom concentration, interacting with dislocations with the temperature increase. Nevertheless, the pinning stress in this state is higher than in the other two pointed states due to the greater number of atoms, which entered into the GBs in the result of the grain volume increase.

Let us analyze the relative contribution of the different pointed out factors into the investigated dependencies $\sigma_y = f(d^{-1/2})$.

The tendency of the yield stress change, conditioned by the microstructure defects, depending on the grain size is presented in Fig. 2. The most imperfect is the NS with *d*=130 nm, obtained by HPT at RT. The least defective is the NS with *d*=210 nm, obtained by HPT at 200 °C. Accordingly, the flow stress conditioned by the crystal lattice defects, in the first case is higher than in the second one. At the same time the contribution of the pinning dislocation stress by the Mg atoms has the opposite tendency (Fig. 2).

Fig. 3 presents the modeling values of the flow limit $\sigma_{0.2}$, obtained according the formula (3) at the strain 0.2% taking into account the contribution of the grain size, dislocations, segregations of the Mg atoms. According to the modeling results the most values of the strength parameters belong to the samples, subjected to HPT at RT. This result agrees with the experimental data according to which $\sigma_{0.2}$ has the highest values for the pointed out state (Table 1). The high values of the mentioned parameters are explained by the grain refinement, the high level of the crystalline lattice defects, attained in the result of HPT and by the pinning of dislocations by the Mg atoms in GBs (Fig. 1, Fig. 2), enumerated in order of decrease of their contribution.

As it follows from the above mentioned results the material yield limit depends not only on the grain size, but on the microstructure peculiarities, developed under various conditions of the sample deformation. At the same time the modeling points describe the experimental dependency $\sigma_y = f(d^{-1/2})$ quite correctly (Fig. 3). However, the modeling points

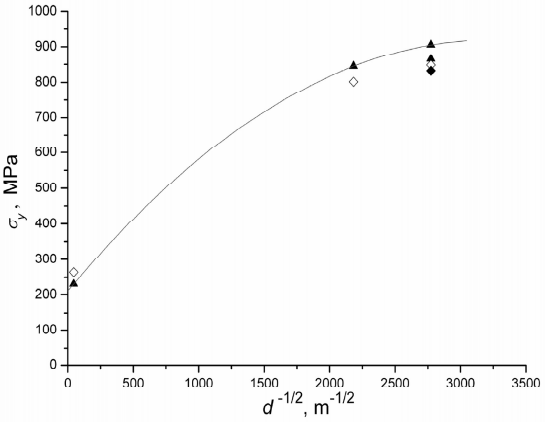

Fig. 3. Dependency of the yield limit σ_y on $d^{-1/2}$: ▲ – the experimental points, ◇ – the correlated model points, calculated according to Eqs. (3), (10), and (12) at the strain degree ε=0.002. The lower experimental point at *d* = 130 nm corresponds to the state after HPT at 100 °C, ◆ – is the corresponding model point.

corresponding to the states after HPT are located a bit lower than the experimental points. The difference between the experimental and model points can be referred to the drag stress, conditioned by the dislocation cutting of the disperse particles of the second phase segregated in the HPT process and solid solution hardening, which were changing depending on the HPT conditions. These factors have not been considered in the model. Their presence must have increased the friction stress σ_0 and bring to the quantitative correspondence between the experimental and model strength values.

The observed experimental dependency $\sigma_y = f(d^{-1/2})$ is non-monotonous. This peculiarity of the HP correlation in case of micron and submicron size microstructures has been pointed out in paper [19]. In the vicinity of the value $d \approx 1$ μm the value of the HP coefficient becomes higher. In case with Al the grain size of the order 1 μm is critical, as the dislocation cell structure does not develop at lower grain sizes. So, the yield stress will be determined by the grain sizes and GBs properties as the sources and sinks for dislocations. The higher HP coefficient value can be explained by the higher density of dislocation sources in GBs [19]. However, according to the modeling results the high-strength states in Al-Mg alloys, subjected to SPD, can be connected not only with the small grain size, but mainly with the dislocation pinning of the Mg atoms, accumu-

lated in the GBs area. They also depend on the density of dislocations.

The analysis of the mentioned above factors, which influence the alloy strength, simultaneously allowed to reveal the ones leading to embrittlement or, conversely, increasing the ductility of the samples under research. The grain size increases along with the temperature increase of the SPD process from 130 nm at RT up to 210 nm at 200 °C. In connection with this, the concentration of the Mg atoms in GBs has increased. The microstructure has become less imperfect at the same time. In the result of modeling it has been specified that high value of the yield limit in this case is attained mainly on account of the dislocation pinning stress by the Mg atoms in the GBs area (Fig. 2).

The states after HPT at 100 °C and 200 °C are defined by further reduction of the strength parameters of an alloy (Fig. 3), which agrees with the experimental data. At the same time, as it follows from the experiment (Table 1), the ductility of the samples decreases too. Besides, the brittle fracture takes place in the samples subjected to HPT at 200 °C at the moment of the beginning of yielding flow [2]. As it follows from the modeling results, the embrittlement of the material is related with the increase of the pinning stress of dislocations τ_s against the low microstructure imperfection (Fig. 2). After HPT at RT the contribution of defects into strength grows, the pinning stress slightly decreases, but still stays higher than the value of dislocation hardening (Fig. 2). As the result the strength increases as well as the ductility.

4. CONCLUSIONS

In the result of the numerical modeling the dependencies $\sigma_y = f(d^{-1/2})$, which adequately describe the experimental data, presented in the form of the HP dependency, have been obtained The modeling has allowed to explain the mechanisms developing the ultrahigh-strength states in NS Al-Mg alloys on the example of the Al 1570 alloy. It turned out that the strength of the viewed samples depends not only on the grain size, but at the same time appears to be the function of microstructure peculiarities, developed in the process of severe thermomechanical material treatment. The ultrahigh-strength states in the Al alloys, obtained by the SPD method, are realized in the result of the segregation of the Mg atoms, leaving the grain bodies for the GB area, and the dislocation pinning by them. The influence of the dislocation density is less intense, especially at higher temperatures. In connection with this the dislocation density growth leads not only to the material hardening increase, but creates the plasticity reserve. The inconsiderable material hardening is realized, possibly, on the account of the trapping of dislocations by the disperse particles, developed in the HPT process, as well as solid solution hardening, which increase the crystal lattice friction stress for the dislocation slip in the sample.

REFERENCES

[1] A. Vinogradov, A. Washikita, K. Kitagawa and V.I. Kopylov // *Mater. Sci. Eng. A* **349** (2003) 318.
[2] M.Yu. Murashkin, A.R. Kil'mametov and R.Z. Valiev // *The Physics of Metals and Metallography* **106** (2008) 90.
[3] D. Witkin, Z. Lee, R. Rodriguez, S. Nutt and E. Lavernia // *Scripta Mater*. **49** (2003) 297.
[4] H. Konrad, In: *Ultrafine Grain in Metals*, ed. by L.K. Gordienko (Metallyrgy: M., 1973), p. 206.
[5] R.V. Armstrong, In: *Ultrafine Grain in Metals*, ed. by L.K. Gordienko (Metallyrgy, Moscow, 1973), p. 7.
[6] N. Hansen // *Scripta Mater*. **51** (2004) 801.
[7] A.H. Chokshi, F. Rozen, J. Karch and H. Gleiter // *Scripta Met.* **23** (1989) 1679.
[8] P.G. Sanders, J.A. Eastman and J.R. Weertman // *Acta Mater.* **45** (1997) 4019.
[9] R.W. Rice, C. Wu, F. Bouchett // J. Am. Ceram. Soc. **77** (1994) 2539
[10] R.Z. Valiev and I.V. Alexandrov, *Nanostructured Materials Obtained by Severe Plastic Deformation* (Logos, Moscow, 2000).
[11] M.V. Markushev and M.Y. Murashkin // *Phys. Met. Metallogr*. **98** (2004) 1.
[12] J.P. Hirt and J. Lothe, In: *Theory of dislocations*, ed. by E.M. Nadgorny and Y.A. Osipyan (Atomisdat, Moscow, 1972).
[13] O. Sitdikov, T. Sakai, E. Avtokratova, R. Kaibyshev, K. Tsuzaki and Y. Watanabe // *Acta Mater*. **56** (2008) 821.
[14] S.M. Klotsman // *Physical Science Success* **160** (1990) 99.
[15] T. Narutani and J. Takamura // *Acta. Met. Mater*. **39** (1991) 2037.
[16] P. Ambrosi, W. Homeier and Ch. Schwink // *Scripta Met*. **14** (1980)183.
[17] W.A. Curtin, D.L. Olmsted and L.G. Hector // *Jr. Nature materials* **5** (2006) 875.
[18] R.Z. Valiev, V.Yu. Gertsman, O.A. Kaibyshev and Sh.K. Khannanov // *Phys. Stat. Sol. (a)* **78** (1983) 177.

[19] G.A. Malygin // *Solid State Physics* **49** (2007) 961.
[20] F.B. Prinz and A.S. Argon // *Acta Metall*. **32** 7 (1984) 1021.
[21] M. Zehetbauer // *Acta mater.* **41** (1993) 589.
[22] I.V. Alexandrov and R.G Chembarisova // *Rev. Adv. Mater. Sci.* **16** (2007) 51.
[23] G.A. Malygin // *Phys. Stat. Sol.* **37** (1995) 2281.
[24] V.Y. Gertsman, V.Z. Bengus, R.Z. Valiev and O.A. Kaibyshev// *Phys. Stat. Sol.* **26** (1984) 1712.
[25] A.P. Sutton and V.Vitek // *Acta Met.* **30** (1982) 2011.
[26] A.D. Le Kler, *Diffusion in Metals with Bulk Centered Lattice* (Metallurgiya: Moscow, 1969).
[27] B.I. Smirnoff, *Dislocation Structure and Crystal Hardening* (Science, Leningrad 1981).
[28] G.A. Malygin // *Phys. Stat. Sol*. **37** (1995) 3.
[29] G.A. Malygin // *Physical Science Success* **169** (1999) 979.
[30] *Aluminum: Properties and Physical Metallurgy*, ed. by J. E. Hatch (AMS, Metals Park: Ohio, 1984).
[31] G. Nurislamova, X. Sauvage, M. Murashkin, R. Islamgaliev and R. Valiev // *Phil. Mag. Lett*. **88**(6) (2008) 459.
[32] R.Z. Valiev, R.K. Islamgaliev and I.V. Alexandrov // *Progr. Mater. Sci.* **45** (2000) 103.
[33] T. Fujita, Z. Horita and T.G. Langdon // *Philos. Mag. A* **82** 11 (2002) 2249.
[34] L.N. Gusev, M.F. Nikitina, L.D. Dolinskaya and I.V. Egiz // *Izv. Akad. Nauk SSSR, Met.* **4** (1972) 208.